Contents list available at CBIORE journal website

International Journal of Renewable Energy Development

Journal homepage: https://ijred.cbiore.id

Research Article

Process optimization in simultaneous saccharification and fermentation system for bioethanol production from Pakchong grass (*Pennisetum purpureum cv Thailand*)

Annisa Septyana Ningrum[a], Erick Rafael Sihombing[a], Satria Ahmadsyah Murdianto[a], Ruri Agung Wahyuono[a,b*]

[a]*Department of Engineering Physcis, Institut Teknologi Sepuluh Nopember, Jl. Arief Rahman Hakim, Sukolilo, 60111, Surabaya, Indonesia*

[b]*School of Interdisciplinary Management and Technology, Institut Teknologi Sepuluh Nopember, Jl. Cokroaminoto 12A, 60264, Surabaya, Indonesia*

Abstract. To support the 2060 Net Zero Emission (NZE) target under the Paris Agreement, increasing the proportion of bioethanol blends to 20-30% has become a national priority. However, limited sugarcane-derived bioethanol production in Indonesia highlights the urgent need for alternative biomass sources. *Pennisetum purpureum cv. Thailand* (Pakchong grass) presents a promising candidate due to its high biomass yield, low lignin content, and adaptability. This study aims to optimize the bioethanol production process from Pakchong grass through pretreatment, enzymatic saccharification, and fermentation, utilizing a modified simultaneous saccharification and fermentation (SSF) scheme. Pretreatment optimization using NaOH (1-5%) revealed that 5% NaOH for 15 minutes effectively removed up to 70% lignin and 78% hemicellulose while retaining 66% cellulose. Enzymatic saccharification using 10 g/L cellulase for 5 days yielded 76.18% glucose conversion without requiring costly additives. Bioethanol fermentation was conducted using six fermentation schemes involving simultaneous (SSF), fed-batch (FSSF), and pre-saccharification strategies (PSFF). Among them, the two-feed FSSF (SE2) produced the highest ethanol yield (32 g/L, 95.41% efficiency), outperforming both conventional SSF (SE1) and PSFF variants. The findings emphasize the importance of synchronizing enzymatic hydrolysis with yeast metabolic activity. This work demonstrates the feasibility of integrated pretreatment and fermentation strategies for bioethanol production from Pakchong grass, offering insights for scalable and cost-effective renewable fuel development in tropical regions.

Keywords: Bioethanol, Fermentation, Pretreatment, Optimization, Pakchong grass

Received: 13th July 2025; Revised: 26th Sept 2025; Accepted: 18th Nov 2025; Available online: 1st Dec 2025

1. Introduction

The Net Zero Emission (NZE) 2060 policy under the Paris Agreement targets a bioethanol blending ratio of 20-30% (IEA, 2022). Indonesia has shown progress through the launch of Pertamax Green 95 (E5) in Surabaya and Jakarta in 2023 (Kumparan, 2023). The Ministry of Energy and Mineral Resources (ESDM) of Indonesia has set a goal to raise bioethanol blending to 10% by 2029 (Presidential Decree, 2023). Achieving this will require approximately 7.3 million kL of ethanol, equivalent to 1.37 million hectares of sugarcane plantations. However, existing sugarcane plantations only produce 40,000 kL per year, representing just 0.55% of the 2029 target (IESR, 2024).

To mitigate the risks associated with land-use change and monoculture expansion, biomass diversification is crucial. One promising alternative is Pakchong grass, which offers high productivity and adaptability. Its dry matter yield can reach 438-500 tons ha^{-1} yr^{-1}, exhibiting superior physical characteristics (Ernawati *et al.,* 2023). As a feedstock, it contains 36-42% cellulose, 19-28% hemicellulose, and 6-12% lignin (Loedkunchotipat *et al.,* 2015; Lounglawan *et al.,* 2014; Pensri *et al.,* 2016; Rengsirikul *et al.*, 2013). The relatively low lignin content facilitates enzymatic hydrolysis, with theoretical yields of 27-31.5% glucose and 9.5-14% xylose (Rahardjo *et al.,* 2021).

Bioethanol production utilizes microbes that ferment sugars into ethanol (Boonchuay *et al.,* 2021). The efficiency of the fermentation process is significantly influenced by the fiber structure and the fermentable sugar content of Pakchong grass (Kongkeitkajorn *et al.,* 2021). In this biomass, cellulose and hemicellulose fibers are surrounded by lignin, which inhibits enzymatic hydrolysis. Therefore, pretreatment is required to reduce lignin content. Pensri *et al.* (2016) reported that NaOH pretreatment reduced lignin content by up to 86.1%, leaving 76.3% cellulose. However, the associated structural and morphological changes remain insufficiently characterized.

Hydrolysis and fermentation can be conducted separately (SHF) or simultaneously (SSF). The SHF method is less efficient due to longer processing times, higher inhibition, and additional operational steps (Olofsson *et al.,* 2008). Conversely, SSF mitigates enzyme inhibition and improves process efficiency but requires microbes with a wider temperature tolerance (Balat, 2011). Afedzi & Parakulsuksatid (2023) reviewed four SSF modifications: pre-SSF (PSSF), fed-batch SSF (FSSF), semi-

* Corresponding author
Email: wahyuono@its.ac.id (R. A. Wahyuono)

https://doi.org/10.61435/ijred.2026.61568
ISSN: 2252-4940/© 2026.The Author(s). Published by CBIORE

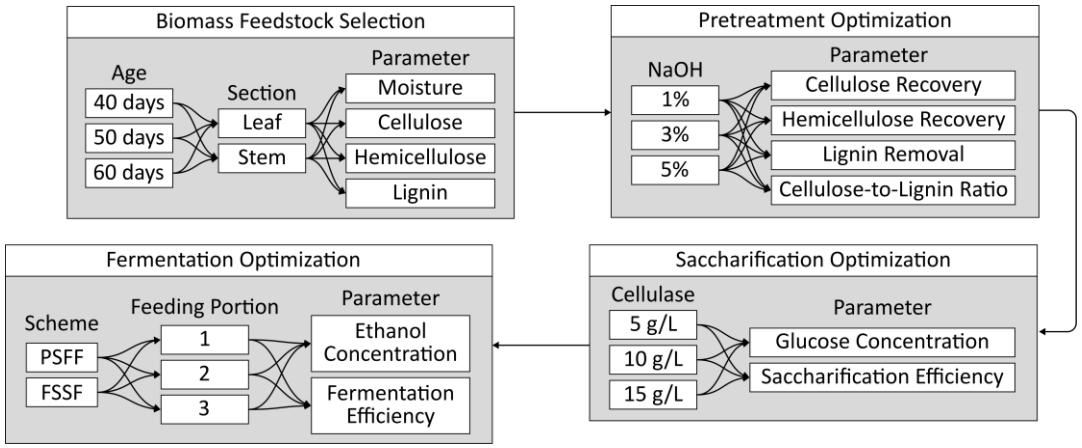

Fig 1. Overall optimization scheme for bioethanol production from Pakchong grass, involving biomass feedstock selection, pretreatment, saccharification, and fermentation optimization.

continuous SSF (SFSS), and co-fermentation SSF (SSCF). Among these, FSSF offers high productivity with lower energy demand. The optimization of modified SSF methods has been widely explored in recent studies using diverse lignocellulosic feedstocks, including oil palm empty fruit bunch (Prasetyo et al., 2025) and sugarcane bagasse (Gao *et al.,* 2018). In this study, pre-saccharification and fed-batch fermentation (PSFF) was developed to sequentially optimize each stage of the fermentation.

Given Indonesia's abundant grass biomass, this study focuses on optimizing Pakchong grass conversion for ethanol production. The optimization process will be conducted in stages by evaluating: (i) biomass composition of Pakchong grass after pretreatment; (ii) periodic changes in glucose concentration during saccharification; and (iiii) efficiency of PSFF and FSSF fermentation schemes in ethanol production.

2. Method

2.1 Materials

Pakchong grass (*Pennisetum purpureum cv. Thailand*), both leaf and stem parts, was harvested 40, 50, and 60 days after planting from a field in Blarang Village, Tutur District, Pasuruan Regency, East Jawa (7°55'04.3"S 112°48'59.9"E). The samples were stored under refrigeration at 4°C.

Chemicals used in this study included sodium hydroxide, 98% sulfuric acid, sodium acetate, acetic acid, D(+)-glucose anhydrous, all obtained from Merck, Germany. The glucose reagent (GOD-PAP) was purchased from Faslab Diagnostics Ltd., Austria and its compositions included phosphate buffer (100 mmol/L), glucose oxidase (>7 U/mL), peroxidase (>0.14 U/mL), phenol (5 mmol/L), and 4-aminoantipyrine (0.5 mmol/L). The cellulase enzyme (10,639 U/g) was sourced from Xi'an Best Bio-Tech Co., Ltd. (Shaanxi, China), and *Saccharomyces cerevisiae* (ATCC 9763, 5×10^8 cfu/mL) from AGAVI Lab (Bandung, Indonesia). Potato dextrose agar (PDA) medium (agar 15 g/L, dextrose 20 g/L, and potato extract, 4 g/L) was obtained from Merck, Germany. An overview of the optimization process for feedstock selection, pretreatment, saccharification, and fermentation is illustrated in Figure 1.

2.2 Biomass Feedstock Selection

Pakchong grass was categorized based on plant age (40, 50, and 60 days) and plant part (leaf and stem). The grass was chopped into 5 mm pieces and oven-dried at 90°C for 5 hours for leaves and 11 hours for stems. Selection was conducted based on cellulose, hemicellulose, and lignin content, determined using the sequential fractionation method of Chesson-Datta as illustrated in Figure 2 (Datta, 1981). All measurements were performed in triplicate to ensure statistical reliability.

2.3 Optimization of Alkali Pretreatment

Before pretreatment, Pakchong grass was chopped to a particle size of approximately 5 mm and oven-dried at 90°C for 5 hours. Pretreatment was performed on 15 g of dried grass using NaOH solutions at 1%, 3%, and 5% (w/v), prepared in distilled water to a total volume of 400 mL. The samples were autoclaved at 120°C for 15 minutes, then washed eight times with distilled water and oven-dried.

A portion of each pretreated sample was analyzed using the Chesson-Datta method to determine the lignocellulosic composition. All measurements were performed in triplicate. The sample with the most favorable composition was further characterized using SEM, XRD, and FTIR. The effectiveness of alkali pretreatment was evaluated based on cellulose recovery, hemicellulose removal, lignin removal, and the cellulose-to-

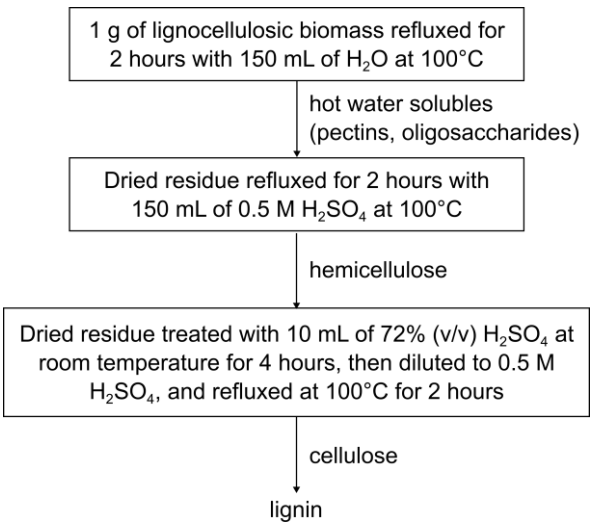

Fig 2. Sequential fractionation of lignocellulose polysaccharides (Datta, 1981).

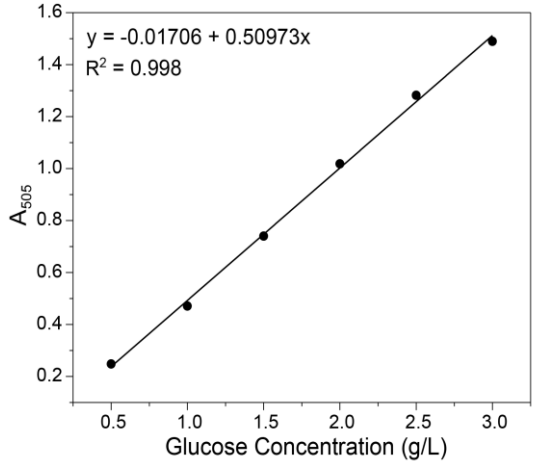

Fig 3. Calibration curve for glucose determination using the GOD-PAP method measured by UV-Vis spectroscopy.

lignin ratio, calculated from the recovered composition and mass after pretreatment.

2.4 Optimization of Cellulose Saccharification

The saccharification process was evaluated based on glucose release over time and cellulose-to-glucose conversion efficiency. A total of 1 g of delignified Pakchong grass was suspended in 10 mL of 1.0 M acetate buffer at pH 5.0. Commercial cellulase enzyme was added at a concentration of 5, 10, and 15 g/L. The mixture was incubated at 50°C on a hotplate magnetic stirrer and manually stirred every 6 hours for 5 days without pH control. Every 6 hours, 1 mL of hydrolysate was withdrawn and stored at 4°C for analysis.

Glucose concentration was determined using the GOD-PAP method. A calibration curve was prepared beforehand, as shown in Figure 3. The hydrolysate samples were centrifuged at 4000 rpm for one hour. Since the upper quantification limit of the glucose oxidase reagent was ten times higher than the sample concentration, the supernatants were diluted tenfold before measurement at 505 nm using a UV-Vis spectrophotometer. All analyses were conducted in triplicate to ensure statistical robustness.

Saccharification efficiency was calculated by comparing the experimental and theoretical conversion of cellulose to glucose. Based on the stoichiometry of cellulose hydrolysis (Equation 1):

$$(C_6H_{10}O_5)_n + nH_2O \rightarrow nC_6H_{12}O_6 \quad (1)$$

According to this reaction, 1 mole of cellulose yields 1 mole of glucose. Therefore, the theoretical maximum yield of glucose from 1 g of cellulose is 1.111 g. Cellulose-to-glucose conversion efficiency was calculated using Equation 2.

$$Efficiency\ (\%) = \frac{Glucose\ yield\ (g)}{Cellulose\ consumed\ (g) \times 1.111} \times 100\% \quad (2)$$

2.5 Optimization of Bioethanol Fermentation

Saccharomyces cerevisiae (5×10^8 cfu/mL) was pre-cultured aerobically on PDA at 30°C for 48 hours. The optimal conditions obtained from the delignification and saccharification were replicated in the fermentation stage to determine the most effective scheme for converting Pakchong grass into ethanol. Optimization was carried out by varying fermentation schemes, feeding strategi es, and microbial ratios, with performance evaluated based on ethanol concentration and conversion efficiency.

Table 1
Composition of the FSSF and PSFF fermentation scheme variations

Fermentation scheme		Substrate (g)	Enzyme (g)	Yeast (mL)
FSSF	SE1	6	0.50	2
	SE2	2×3	2×0.25	2
	SE3	3×2	3×0.167	2
PSFF	S1	6	0.50	2
	S2	2×3	0.50	2
	S3	3×2	0.50	2

Glass vials (50 mL) were used as small-scale reactors. The yeast culture was diluted to 5×10^4 cfu/mL in 50 mM acetate buffer solution (pH 4.8), following Yasuda et al. (2014). Fermentation was performed under two schemes, PSFF and FSSF, both designed for ethanol production.

In the PSFF scheme, saccharification was conducted first using the optimal cellulase concentration determined previously. After 4 days, additional substrate was added in varying amounts within the same reactor before initiating fermentation. In contrast, FSSF involved simultaneous saccharification and fermentation. Details of all six fermentation variations are listed in Table 1, including:

(i) SE1, basic SSF with single-dose substrate and enzyme, fermented for 7 days;
(ii) SE2, FSSF with substrate and enzyme split into two equal portions at 0 and 24 hours, then fermented for 6 more days;
(iii) SE3, FSSF with three feedings at 0, 24, and 48 hours, followed by 5 days of fermentation;
(iv) S1, PSFF with pre-saccharification for 4 days, followed by 3 days of fermentation;
(v) S2, PSFF with substrate fed in two equal portions at 0 and 24 hours, pre-saccharified for 3 days, then fermented for 3 more days;
(vi) S3. PSFF with three feedings at 0, 24, and 48 hours, hydrolyzed for 2 days, then fermented for 3 days.

Ethanol content was measured using a glass alcoholometer (Alla France, N Tralles, calibrated at 20°C). Samples were first distilled (AOAC/TTB distillation procedure) to separate ethanol from non-volatile solutes. The distillate was allowed to reach the hydrometer's calibrated temperature. Each analysis was carried out in triplicate to ensure reproducibility. The conversion efficiency is calculated based on the molar mass values of glucose (180 g/mol) and ethanol (46 g/mol). The glucose fermentation reaction is shown in Equation (3):

$$C_6H_{12}O_6 \rightarrow 2C_2H_5OH + 2CO_2 \quad (3)$$

According to this reaction, 1 mole of glucose will be converted into 2 moles of ethanol. Thus, theoretically every 1 g of glucose can produce a maximum mass of ethanol of 0.511 g. Therefore, the calculation of the efficiency of converting glucose into ethanol is as follows:

$$Efficiency\ (\%) = \frac{Ethanol\ yield\ (g)}{Glucose\ consumed\ (g) \times 0.511} \times 100\% \quad (4)$$

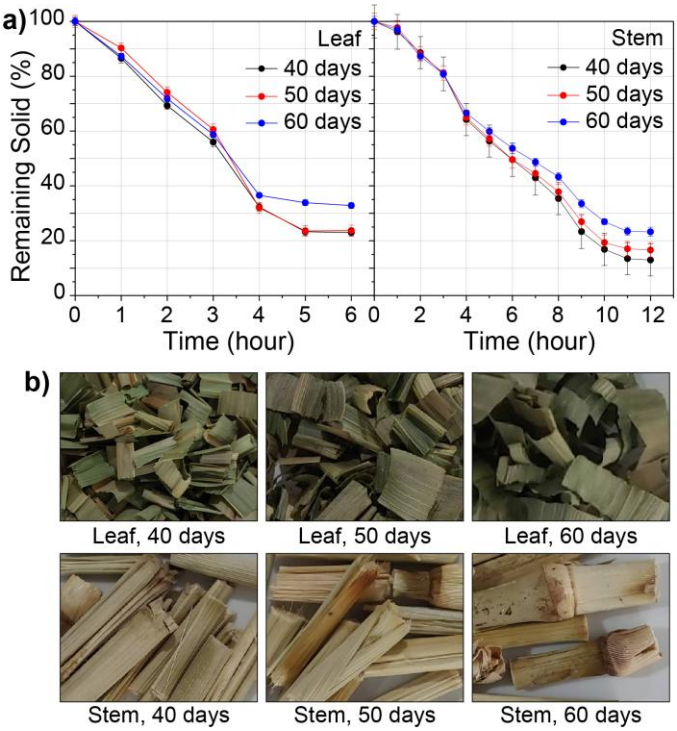

Fig 4. Percentage of remaining solid mass of stem and leaf samples at different plant ages (40, 50, and 60 days) during oven drying and visual appearance of leaf and stem samples after drying.

Table 2
Moisture and lignocellulosic composition (cellulose, hemicellulose, and lignin) of Pakchong grass leaves and stems across harvest ages of 40, 50, 60 days

Section	Age (days)	Moisture (%)	Cellulose (%)	Hemicellulose (%)	Lignin (%)
Leaf	40	77.00	39.52	44.97	13.74
	50	76.29	32.22	48.66	16.51
	60	65.71	24.05	51.02	21.58
Stem	40	87.13	31.14	49.49	17.32
	50	83.67	21.43	58.13	18.90
	60	76.07	17.88	49.46	31.72

3. Results and Discussion

3.1 Biomass Characteristics of Pakchong Grass

Pakchong grass exhibits different characteristics between its leaf and stem fractions. However, variations in harvest age did not significantly affect overall moisture content. The percentage of remaining solid mass of stem and leaf samples during oven drying is shown in Figure 4. Based on the data in Table 2, moisture content tended to decrease as the plants matured. In general, the moisture content of grasses exceeds 60% (Ernawati *et al.,* 2023), resulting in relatively low dry mass yields. The leaves of Pakchong grass had a higher dry mass than the stems.

In this study, Pakchong grass was dominated by hemicellulose, differing from previous reports that identified cellulose as the major component (Manokhoon & Rangseesuriyachai, 2020; Pensri et al., 2016; Phitsuwan *et al.,* 2016). However, those studies did not specify the plant parts or harvest ages of their samples. A biogasification study on Pakchong grass harvested at 35-55 days showed a similar pattern to this research, with hemicellulose as the predominant fraction (Chanpla *et al.,* 2018).

The leaves of Pakchong grass demonstrated better characteristics compared to the stems, with higher cellulose and lower lignin content. Evidence of lignification was observed at 60 days, marked by a significant increase in lignin levels. Biomass that has undergone lignification is less suitable for bioethanol production due to reduced saccharification efficiency (Kongkeitkajorn *et al.,* 2021). Considering its high cellulose content and low lignin level, leaves harvested at 40 days were selected as the feedstock for subsequent processes.

3.2 Effect of Alkali Pretreatment on Chemical Composition of Pakchong Grass

The lignocellulosic composition of Pakchong grass after alkali pretreatment is shown in Figure 5. Cellulose content increased significantly with higher NaOH concentrations, from 39.52% in untreated biomass to 64.63% after 5% NaOH treatment. Hemicellulose content decreased from 44.98% to 24.58%, while lignin content declined slightly from 13.74% to 10.27%.

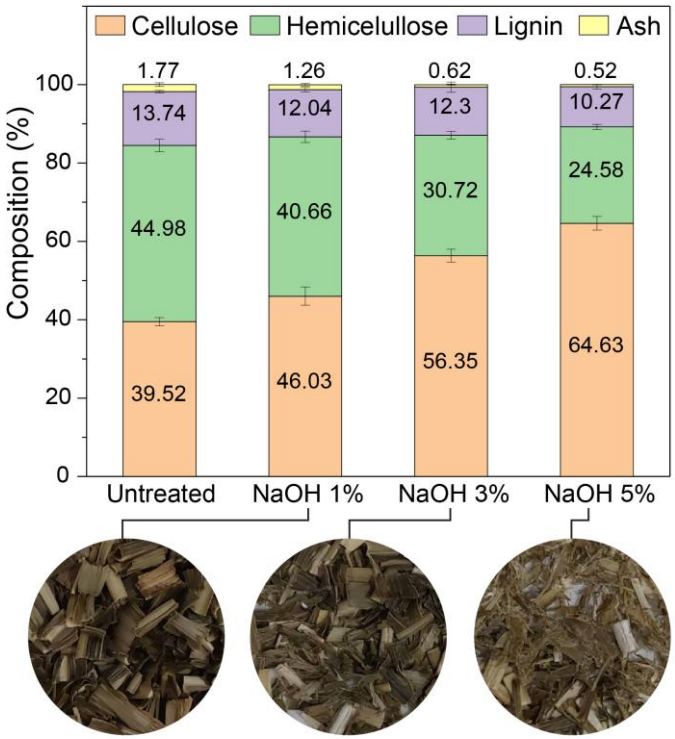

Fig 5. Lignocellulosic composition before and after alkali pretreatment and visual appearance of pretreated leaf samples of Pakchong grass.

Table 3
Lignocellulosic composition of alkali pretreated Pakchong grass based on remaining solids after pretreatment

NaOH concentration (% w/v)	Solid recovery (%)	Cellulose recovery (%)	Hemicellulose removal (%)	Lignin removal (%)	Cellulose/Lignin
1	85.08	99.10	23.08	25.42	3.82
3	48.71	69.46	66.73	56.38	4.58
5	40.47	66.18	77.88	69.75	6.28

As presented in Table 3, pretreatment with 3% and 5% NaOH removed more than 50% of the dry mass, leaving 48.71% and 40.47% of it, respectively. Although about half of the mass was lost, the relatively stable cellulose content during pretreatment suggests that NaOH selectively removed lignin and hemicellulose without significant cellulose degradation.

Lignin removal exceeded 50% when using at least 3% NaOH, indicating effective delignification and an overall improvement in biomass quality compared to untreated samples. Among all treatments, 5% NaOH achieved the highest lignin removal while maintaining cellulose recovery similar to 3% NaOH. While the 5% NaOH treatment caused a decrease of 8.24% in solid recovery and 3.3% in cellulose recovery, it improved hemicellulose and lignin removal to 11.15% and 13.37%, yielding a cellulose-to-lignin ratio of 6.28.

According to Table 4, Pensri et al. (2016) achieved the highest lignin removal (89.9%) and the highest cellulose recovery (85%) using 3% NaOH at 121°C for 60 minutes, which is relatively longer than this study. Manokhoon & Rangseesuriyachai (2020) also obtained good delignification (80.3%) with moderate cellulose recovery under similar conditions. Minmunin *et al.* (2015) reported high solid recovery (76.5%) and cellulose recovery (79.7%) using 5.5% NaOH at 70°C for 2 hours, but lignin removal was only 53.4% demonstrating a trade-off between yield and delignification.

In contrast, this study achieved 69.75% lignin removal within only 15 minutes at 120°C, with moderate solid recovery (40.5%) and cellulose recovery (65.4%), representing a practical balance between speed and selectivity. The short pretreatment duration offers a clear advantage by reducing energy consumption and process bottlenecks. For comparison, Camesasca *et al.* (2015) used a two-stage acid-alkali pretreatment lasting 7 hours, achieving similar lignin removal (68.9%) but at the expense of longer processing and higher chemical usage.

3.3 Effect of Alkali Pretreatment on Functional Groups

FTIR characterization was conducted to identify changes in lignocellulose-related bond signals. Spectra within the wavenumber range of 500-4000 cm^{-1} were analyzed to determine the functional groups in the samples before and after pretreatment. The spectra are shown in Figure 6 and the corresponding band assignments are summarized in Table 5.

The peaks at 3342 cm^{-1} and 2919-2852 cm^{-1} correspond to O-H and aliphatic C-H stretching vibrations, primarily derived from cellulose and hemicellulose. These peaks remained prominent across all pretreated samples, consistent with the composition of pretreated grass in Figure 5, which shows similar sum of cellulose and hemicellulose content after pretreatment.

Table 4
Comparison of lignocellulosic composition and removal/recovery ratios of pretreated Pakchong grass with previous studies. Parameters shown include cellulose (Cel), hemicellulose (Hem), and lignin (Lig) content before and after pretreatment, as well as solid recovery (SR), cellulose recovery (CR), hemicellulose removal (HR), lignin removal (LR), and cellulose-to-lignin ratio (C/L).

Pretreatment	Untreated composition (%)			Pretreated composition (%)			Removal or recovery ratio (%)					Reference
	Cel	Hem	Lig	Cel	Hem	Lig	SR	CR	HR	LR	C/L	
5% NaOH at 120°C for 15 min	40.2	45.8	14.0	65.0	24.7	10.3	40.5	65.4	78.2	70.1	6.3	This work
3% NaOH at 121°C for 60 min	55.6	16.3	28.1	81.9	4.2	13.9	39.9	58.7	89.7	80.3	5.9	Manokhoon *et al*, 2020
3% NaOH at 121°C for 60 min	57.1	33.5	9.4	85.0	12.4	2.6	36.7	54.7	86.5	89.9	32.9	Pensri *et al*, 2016
1.5% H_2SO_4 at 121°C for 60 min and followed by 2% NaOH at 80°C for 6 h	44.1	22.6	33.3	63.7	11.0	25.3	41.0	59.3	80.1	68.9	2.5	Camesasca *et al*, 2015
5.5% NaOH at 70°C for 2 hr	65.3	25.8	8.9	68.1	26.5	5.4	76.5	79.7	21.3	53.4	12.6	Minmunin *et al*, 2015

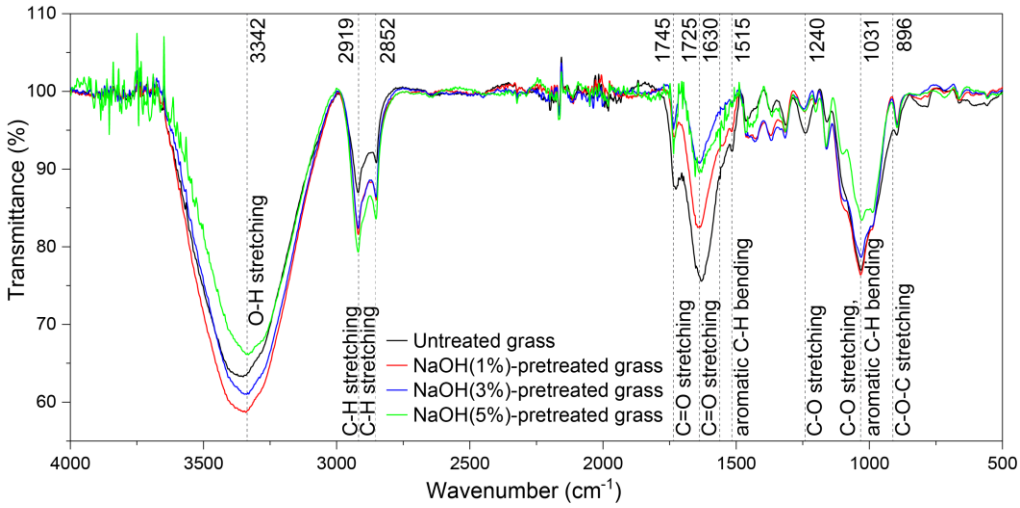

Figure 6. FTIR spectra of Pakchong grass before and after alkaline pretreatment and corresponding functional groups

Carbonyl stretching peaks at 1745, 1725, and 1630 cm^{-1}, typically associated with acetyl side chains of hemicellulose and the aromatic structure of lignin (Faix, 1991; Pandey & Pitman, 2003), were most intense in the untreated sample. Their significant decline after 3% and 5% NaOH pretreatment indicates substantial removal of hemicellulose and lignin.

Similarly, the 1515 cm^{-1} peak (aromatic C-H in-plane bending) and the 1240 cm^{-1} band (C-O stretching of ether bonds in lignin and ester groups in hemicellulose) (Sun et al., 2000) both decreased with increasing NaOH concentration. The greater reduction in the 3% and 5% NaOH samples compared to 1% further supports enhanced delignification at higher alkali level.

A clear decline in intensity was also observed at 1031 cm^{-1}, linked to aromatic skeletal vibrations of lignin (Bergamasco *et al*., 2023), reflecting a consistent reduction in lignin content from untreated to 5% NaOH-treated samples. Meanwhile, the 896 cm^{-1} band, assigned to β-glycosidic C-O-C linkages in cellulose and hemicellulose (Xie *et al.,* 2010), remained relatively unchanged, indicating preservation of carbohydrate structure.

In summary, pretreatment with 3% and 5% NaOH effectively reduced lignin and hemicellulose-related functional groups while preserving cellulose integrity. These spectral trends are consistent with the Chesson-Datta compositional data and confirm that delignification was most effective at higher NaOH concentrations. However, some functional groups (e.g., cellulose vs hemicellulose O-H or C-O signals) have overlapping peaks and cannot be fully resolved by FTIR alone, which is a common limitation in biomass (Kacuráková & Wilson, 2001; Schwanninger *et al.,* 2004).

3.4 Effect of Alkali Pretreatment on Cellulose Crystallinity

XRD analysis was conducted to identify the presence and structural changes of cellulose and hemicellulose in Pakchong grass before and after alkali pretreatment. The diffraction patterns and variations in relative intensity ratios between cellulose and hemicellulose peaks at different NaOH concentrations are shown in Figure 7. As shown in Figure 7(a), four main diffraction peaks were observed: 15.0° and 22.5°, corresponding to the amorphous and crystalline regions of cellulose; and 18.2° and 24.3°, associated with hemicellulose-rich amorphous domains (Meraj *et al.,* 2024).

Changes in the relative intensities of these peaks (Figure 7(b)) quantitatively reflect structural modifications in the lignocellulosic matrix due to pretreatment. The increasing peak ratio with higher NaOH concentrations indicates effective hemicellulose removal without significant cellulose loss. This trend aligns with the compositional results obtained using the Chesson-Datta method.

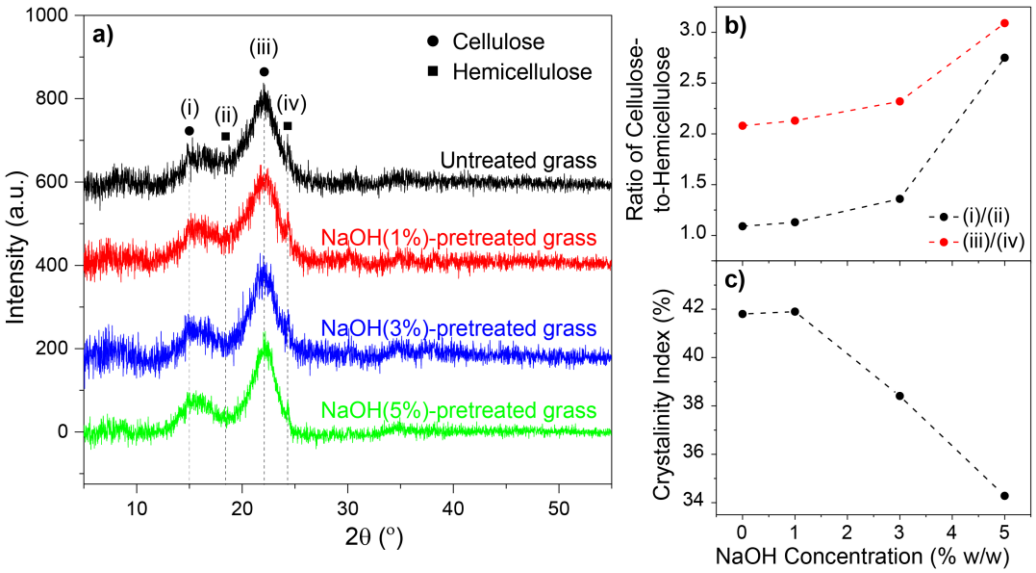

Fig 7. (a) XRD patterns of Pakchong grass before and after alkaline pretreatment and changes in **(b)** cellulose-to-hemicellulose intensity ratio with NaOH concentration as well as **(c)** cellulose crystallinity index before and after alkaline pretreatment with varying NaOH concentrations.

Table 5
Identification of vibration modes and corresponding components in the FTIR spectra of Pakchong grass as reported in previous studies

No.	Wavenumber (cm^{-1})	Vibration mode	Components
1	3342	O-H stretching	Cellulose^{+}, hemicellulose^{+}, lignin
2	2919, 2852	C-H stretching	Cellulose^{+}, hemicellulose^{+}, lignin
3	1725, 1745, 1630	C=O stretching	Hemicellulose, lignin^{+}
4	1515	C-H in-plane bending	Lignin
5	1240	C-O stretching	Lignin
6	1031	aromatic C-H in-plane deformation	Cellulose, lignin^{+}
7	896	C-O-C stretching	Cellulose, hemicellulose

Source: (Cheng et al., 2016; Lara-Serrano et al., 2019; Lun et al., 2017; Meraj et al., 2024; Raspolli Galletti et al., 2015; Zhuang et al., 2020)

To further assess the impact of pretreatment on enzymatic accessibility, the crystallinity index (*CrI*) was calculated and shown in Figure 7(c). Cellulose with high crystallinity typically resists enzymatic hydrolysis due to its dense crystalline regions, whereas decreased crystallinity enhances porosity and enzyme accessibility (Manokhoon & Rangseesuriyachai, 2020).

In this study, the *CrI* of untreated grass was 41.8% and remained nearly unchanged after 1% NaOH pretreatment (41.9%). A notable decrease occurred at 3% NaOH (38.41%), followed by a further reduction to 34.28% at 5%. These results confirm that NaOH concentrations ≥3% effectively disrupted the crystalline structure of cellulose, improving its susceptibility to enzymatic hydrolysis in saccharification process.

3.5 Effect of Alkali Pretreatment on Morphological Structure

The morphological changes in Pakchong grass before and after alkali pretreatment are illustrated in Figure 8. In the untreated sample, the surface appeared compact, with cellulose fibers tightly encapsulated within a hemicellulose-lignin matrix. This structure represents the native integrity of lignocellulose biomass, where components are strongly interlinked.

After pretreatment, particularly at NaOH concentrations ≥3%, the surface morphology changed significantly. At 750× magnification, the fibers appeared more porous and fragmented, with lignin disrupted and unevenly distributed. The

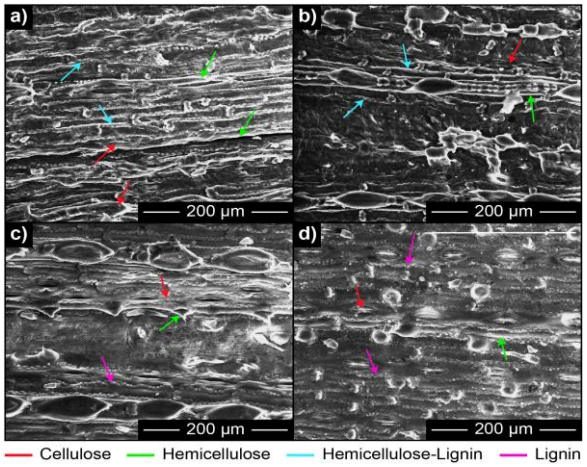

Fig 8. SEM images of Pakchong grass at 750× magnification: **(a)** untreated; and pretreated with **(b)** 1% NaOH, **(c)** 3% NaOH, and **(d)** 5% NaOH.

loss of the hemicellulose-lignin binding matrix indicates that alkaline treatment successfully released hemicellulose and lignin fractions from cellulose.

Higher magnification (5000×) of SEM images in Figure 9 revealed detailed lignin structural changes across treatments. In

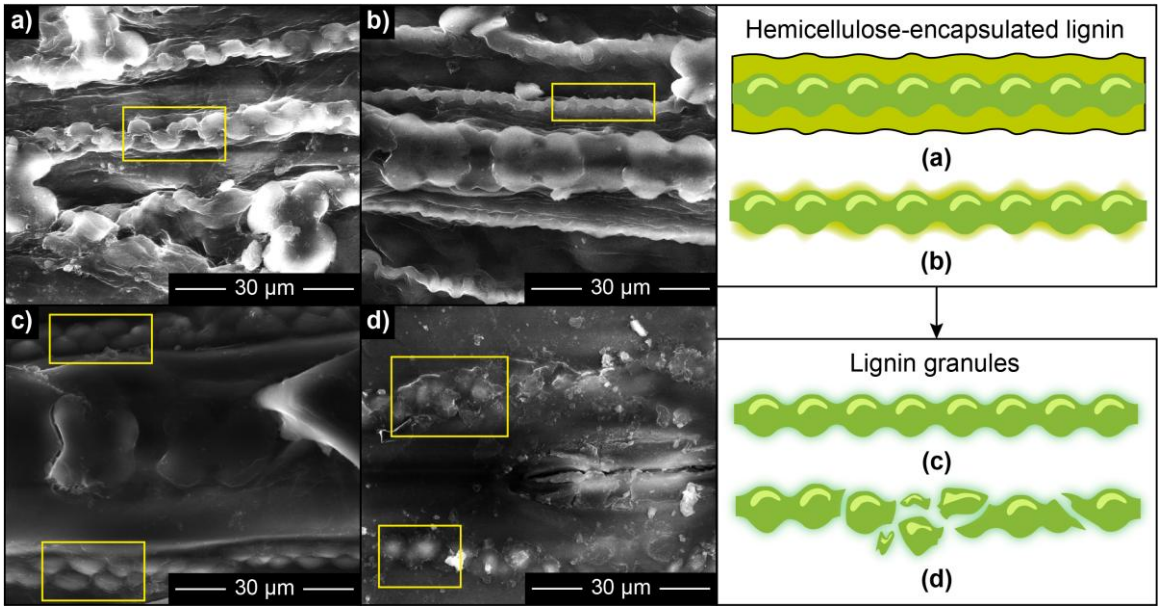

Fig 9. SEM images of Pakchong grass at 5000× magnification: **(a)** untreated; and pretreated with **(b)** 1% NaOH, **(c)** 3% NaOH, and **(d)** 5% NaOH

Table 6
Glucose concentration and saccharification efficiency of cellulose from Pakchong grass at different cellulase concentrations

Cellulase concentration (g/L)	Glucose concentration (g/L)	Saccharification rate (g/L/h)	Glucose yield (g/g biomass)	Conversion efficiency (%)
5	31.177	0.17970	0.3114	43.416
10	54.703	0.30646	0.5469	76.177
15	56.723	0.42933	0.5671	78.990

untreated samples, lignin appeared as interwoven strands, indicating its association with hemicellulose in the lignin-hemicellulose complex (Tarasov et al., 2018). The illustration in Figure 9 (right) shows that with 1% NaOH treatment, the hemicellulose layer surrounding lignin began to thin. With 3% NaOH pretreatment, lignin started to become exposed, and at 5% NaOH concentration, the lignin structure began to break down. These changes opened up access for cellulase enzymes to more easily penetrate the lignin layer and reach the cellulose during the saccharification process.

3.6 Effect of Cellulase Concentration on Glucose Production

Based on the stoichiometry of cellulose hydrolysis, 1 g of cellulose theoretically yields 1.111 g of glucose. In this study, 1 g of NaOH-pretreated Pakchong grass contained 0.6463 g cellulose, with a maximum theoretical glucose yield of 0.7181 g (71.81 g/L) in 10 mL solution. As shown in Figure 10, hydrolysis dynamics varied with cellulase concentration.

According to Table 6, at 5 g/L cellulase, saccharification followed a linear trend with an average rate of 0.1797 g/L per hour, reaching 43.42% of the theoretical yield. However, the relatively low conversion efficiency suggests that this enzyme dosage was insufficient to complete hydrolysis. At 10 g/L cellulase, glucose accumulation displayed a reversed exponential slowdown during the first 100 hours. The initially high glucose concentration likely caused product inhibition, as limited stirring (every six hours) allowed glucose to accumulate around cellulose particles, hindering enzyme access (Shadbahr *et al.,* 2017). After 108 hours, glucose levels increased significantly, reaching 54.7 g/L or 76.18% of the theoretical yield, once diffusion redistributed the glucose and reduced local inhibition effects.

Meanwhile, at 15 g/L cellulase, a similar slowdown was observed during the initial 80 hours. Although this treatment produced a 2.8% higher yield than 10 g/L, the 50% increase in enzyme use made it less efficient from a cost standpoint. Thus, a dosage of 10 g/L cellulase (7.15 FPU or 10.79 FPU/g) for five

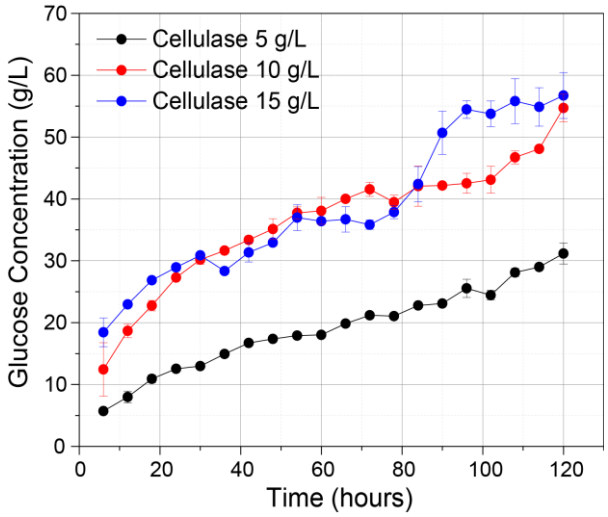

Fig 10. Time-dependent glucose concentration during saccharification with cellulase concentrations of 5 g/L, 10 g/L, and 15 g/L.

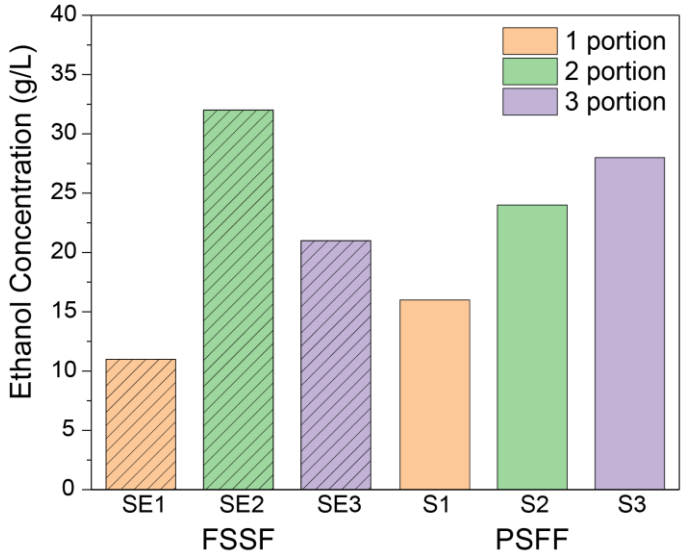

Fig 11. Comparison of ethanol concentrations from PSFF and FSSF schemes with different feeding portions.

Table 7
Ethanol concentration and fermentation efficiency of Pakchong grass in different PSFF and FSSF fermentation schemes

Fermentation scheme		Ethanol concentration (g/L)	Ethanol yield (g/g glucose)	Conversion efficiency (%)
FSSF	SE1	11	0.167	32.79
	SE2	32	0.487	95.41
	SE3	21	0.320	62.61
PSFF	S1	16	0.244	47.70
	S2	24	0.366	71.56
	S3	28	0.426	83.48

days was determined to be the optimal balance between yield and resource utilization, producing 546.9 mg glucose per g biomass.

These findings are comparable with previous studies on lignocellulosic biomass. Pensri et al. (2016) reported 522 mg/g glucose yield using 50 FPU of cellulase at 10% total solids, while Kongkeitkajorn et al. (2021) obtained 70 g/L glucose using 40 FPU/g at 15% total solids. Yasuda et al. (2014) achieved 67% saccharification efficiency using *Acremonium cellulolyticus* on LMAA-pretreated Napier grass, while Panakkal et al. (2022) reported a higher yield of 87.09% using Cellic® Ctec2 enzyme. Camesasca et al. (2015) further enhanced hydrolysis by adding β-glucosidase and PEG 6000, achieving 27 g/L glucose (45% conversion). Although higher yields were often achieved with more potent enzyme formulations or enzyme cocktails, the approach used in this study remains advantageous for its lower enzyme loading requirement and simplified process conditions.

3.7 Optimum Fermentation Scheme

Fermentation performance was evaluated based on ethanol concentration and efficiency relative to theoretical yield (Table 7). Six fermentation strategies were tested, including single- and multi-feed variants of both FSSF and PSFF systems, with durations adjusted to match enzymatic hydrolysis dynamics (Figure 11) and yeast metabolic adaptation.

The SE1 scheme, involving a single substrate and enzyme feeding followed by seven days of fermentation, produced the lowest ethanol concentration (11 g/L, 32.8% of theoretical). Despite its high initial enzyme and substrate loading, SE1 showed clear glucose accumulation within the first 24 hours, likely causing osmotic stress in yeast adapting to anaerobic conditions (Chang *et al.,* 2018). The imbalance between hydrolysis and fermentation rates also contributed to feedback inhibition on both yeast and enzyme activity (Hung *et al.,* 2023, 2025; Pendse *et al*., 2023). As a conventional SSF setup, SE1 was the least efficient due to poor synchronization between peak enzyme activity and yeast adaptation.

In contrast, SE2, the two-feed FSSF variant (0 and 24 hours), achieved the highest ethanol concentration (32 g/L, 95.4% of theoretical). This configuration enabled gradual saccharification and fermentation, allowing yeast to adapt and maintain metabolic activity (Wang *et al.,* 2013). Enzyme performance remained stable through balanced substrate availability and reduced local glucose accumulation (da Silva et al., 2020). This result also confirmed the compatibility of *T. reesei*-derived cellulase with *S. cerevisiae* fermentation at room temperature. The 24-hour feeding interval aligned with the period of fastest enzymatic hydrolysis and active yeast metabolism.

Interestingly, SE3, which introduced three feedings (0, 24, and 48 hours), yielded lower ethanol levels (27.2 g/L, 81.1% efficiency) despite identical total enzyme and substrate amounts. This reduced yield is attributed to limited glucose during the yeast's peak metabolic window (6-24 hours), thus limiting fermentation productivity (Hoyer *et al.,* 2010). Since yeast cannot sustain maximum ethanol production indefinitely, extending feeding beyond this window likely reduced efficiency (Kottelat *et al.,* 2021; Xiao *et al.*, 2025). The decrease in yield may also reflect underutilized enzyme potential and early yeast

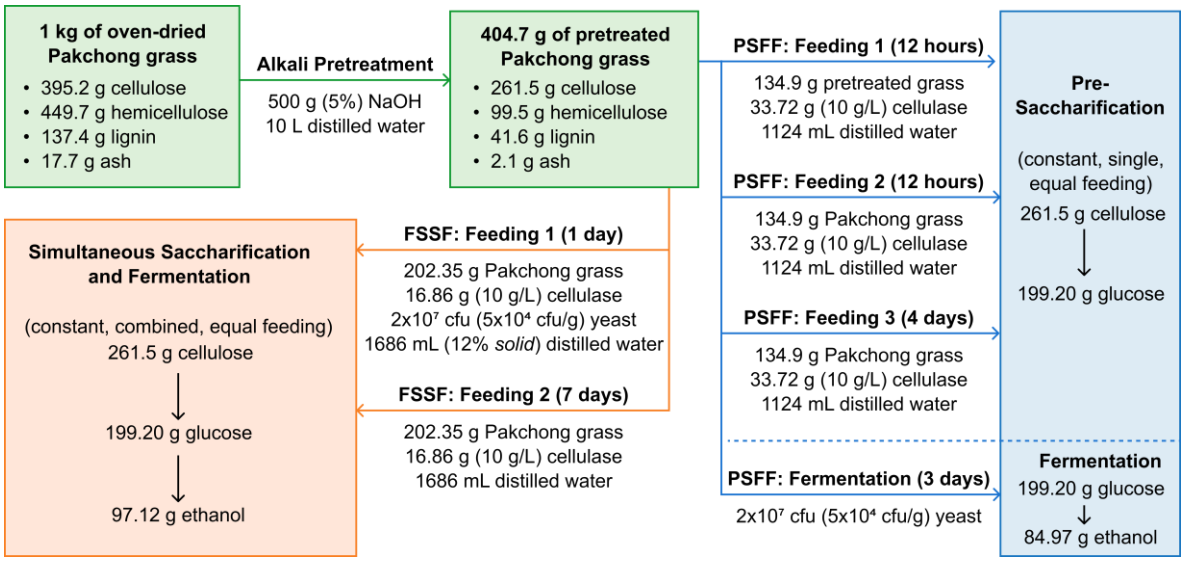

Fig 12. The mass balance analysis for bioethanol production from Pakchong grass using the FSSF and PSFF schemes.

Table 8
Comparison of process and total efficiency between theoretical approach, FSSF, and PSFF fermentation scheme

Simulation approach	Fermentation efficiency (%)	Total efficiency (%)
Theoretical	36.68	14.85
FSSF	23.99	9.71
PSFF	20.99	8.50

deactivation when glucose supply becomes too diluted (Liu et al., 2016).

For PSFF schemes, where pre-saccharification precedes fermentation, S1 achieved 50% higher ethanol concentration than SE1 (16.6 g/L vs. 11 g/L), confirming that pre-saccharification in SSF significantly improves glucose availability and fermentation stability. S1 involved four days of hydrolysis followed by three days of fermentation. Residual enzymes in the reactor continued hydrolysis during fermentation, enhancing conversion (Hoyer et al., 2010). This suggests that partially decoupling hydrolysis from fermentation helps reduce osmotic stress while preserving enzymatic activity.

The substrate-fed PSFF variants (S2 and S3) demonstrated progressively higher ethanol yields with increased feedings. S3, which applied three substrate additions (0, 24, and 48 hours) after two days of hydrolysis, achieved 28 g/L (83.5% efficiency). Unlike FSSF, PSFF variations only delayed substrate addition, without further enzyme feeding during fermentation, which is beneficial since excess free enzyme can inhibit yeast fermentation (Battista *et al.,* 2019; Kristensen *et al.,* 2009; Podkaminer *et al.,* 2012). Gradual substrate feeding also reduced medium viscosity, ensuring smoother glucose release and minimizing fermentation bottlenecks (Fornazier et al., 2025).

Although S3 did not surpass SE2, its consistent yield improvement across feeding stages suggests strong potential for continuous fermentation optimization. These findings indicate that: (i) SE2 is optimal for batch or semi-batch configurations with limited enzyme and yeast; (ii) PSFF with multiple substrate feedings (S3) is more suitable for continuous fermentation systems; (iii) enzyme-only feeding does not enhance fermentation yield, while substrate-only feeding improves it without increasing enzyme cost; and (iv) yeast activity peaks between 6-24 hours post-inoculation, emphasizing the importance of precise glucose supply timing.

In this study, the highest ethanol concentrations reached 32 g/L under the FSSF scheme and 28 g/L under the PSFF scheme. Prasetyo *et al.* (2025) investigated oil palm empty fruit bunch and optimized each process similar to this study, achieving 40 g/L ethanol from both FSSF and PSSF. Gao *et al.* (2018) also applied process optimization using the PSFF scheme on sugarcane bagasse and obtained a higher yield of 75.57 g/L, mainly due to the favorable composition of the biomass. In comparison, Kongkeitkajorn *et al.* (2021) reported 28.5 g/L ethanol from Pakchong grass using a simple SSF scheme. These comparisons indicate that the PSFF modification can improve fermentation efficiency, although the ethanol yield remains strongly influenced by the characteristics of the biomass feedstock.

The mass balance for ethanol production (Figure 12) was calculated from 1 kg of fresh Pakchong grass leaves (40 days). After pretreatment with 10 L of 5% NaOH, 404.7 g of solid biomass remained, containing 261.5 g cellulose. Based on a saccharification efficiency of 76.2% and theoretical conversion stoichiometry, this equates to 199.2 g glucose, corresponding to 101.7 g theoretical ethanol. In the SE2 (FSSF) scheme, this yielded 97.1 g ethanol (95.4% efficiency), while S3 (PSFF) produced 84.97 g ethanol (83.5% efficiency). These correspond to process efficiencies of 23.99% (SE2) and 21.0% (S3), with overall efficiencies of 9.71% and 8.5%, respectively, when calculated per raw biomass (Table 8).

While SE2 was more efficient under batch configuration, S3 demonstrated better potential for scale-up due to its compatibility with continuous feeding and reduced yeast stress. The comparison between FSSF and PSFF schemes highlights the importance of synchronizing saccharification and

fermentation timing, as well as how substrate feeding and enzyme dynamics collectively determine ethanol yield.

4. Conclusion

This study confirms Pakchong grass as a promising feedstock for bioethanol production through an integrated bioconversion strategy. Alkaline pretreatment with 5% NaOH for 15 minutes was optimal for enhancing cellulose accessibility while minimizing processing time. Enzymatic saccharification using 10 g/L cellulase for five days provided the highest glucose yield (76.18%), with higher enzyme doses offering minimal additional benefit. Among six fermentation schemes, the two-feed FSSF (SE2) showed the best ethanol yield (32 g/L), achieving 95.41% of theoretical conversion and 23.99% process efficiency. In contrast, PSFF strategies such as S3 provided more stable fermentation under continuous substrate input, though with slightly lower yield. The findings highlight that yeast activity peaks within 6-24 hours post-inoculation, making timely glucose availability critical. Gradual substrate feeding proved more beneficial than combined enzyme-substrate feeding during fermentation. Future work should investigate scale-up scenarios for FSSF, explore enzymatic recycling, and assess continuous fermentation models to further improve economic and operational viability.

Acknowledgments

The authors extend their gratitude to the Department of Engineering Physics, Faculty of Industrial Technology and Engineering Systems, Institut Teknologi Sepuluh Nopember (ITS) for providing research facilities during the research period.

Author Contributions: A.S.N.: conceptualization, methodology, visualization, formal analysis, investigation, data curation, writing—original draft E.R.S.; investigation, data curation, S.A.M.; investigation, data curation, R.A.W.; supervision, funding acquisition, visualization, project administration, validation, writing—review and editing. All authors have read and agreed to the published version of the manuscript.

Funding: This research was funded by the Directorate of Research, Technology, and Community Service, Directorate General of Higher Education, Research, and Technology, Ministry of Education, Culture, Research, and Technology of the Republic of Indonesia, under contract No. 1137/PKS/ITS/2025. The authors gratefully acknowledge the financial support that made this research possible.

Conflicts of Interest: The authors declare that there are no conflicts of interest regarding the publication of this paper. All funding and support received have not influenced the design, execution, or conclusions.

References

Afedzi, A. E. K., & Parakulsuksatid, P. (2023). Recent advances in process modifications of simultaneous saccharification and fermentation (SSF) of lignocellulosic biomass for bioethanol production. *Biocatalysis and Agricultural Biotechnology*, *54*, 102961. https://doi.org/10.1016/j.bcab.2023.102961

Balat, M. (2011). Production of bioethanol from lignocellulosic materials via the biochemical pathway: A review. *Energy Conversion and Management*, *52*(2), 858–875. https://doi.org/10.1016/j.enconman.2010.08.013

Battista, F., Gomez Almendros, M., Rousset, R., & Bouillon, P.-A. (2019). Enzymatic hydrolysis at high lignocellulosic content: Optimization of the mixing system geometry and of a fed-batch strategy to increase glucose concentration. *Renewable Energy*, *131*, 152–158. https://doi.org/10.1016/j.renene.2018.07.038

Bergamasco, S., Zikeli, F., Vinciguerra, V., Sobolev, A. P., Scarnati, L., Tofani, G., Scarascia Mugnozza, G., & Romagnoli, M. (2023). Extraction and Characterization of Acidolysis Lignin from Turkey Oak (Quercus cerris L.) and Eucalypt (Eucalyptus camaldulensis Dehnh.) Wood from Population Stands in Italy. *Polymers*, *15*(17), 3591. https://doi.org/10.3390/polym15173591

Boonchuay, P., Techapun, C., Leksawasdi, N., Seesuriyachan, P., Hanmoungjai, P., Watanabe, M., Srisupa, S., & Chaiyaso, T. (2021). Bioethanol Production from Cellulose-Rich Corncob Residue by the Thermotolerant *Saccharomyces cerevisiae* TC-5. *Journal of Fungi*, *7*(7), 547. https://doi.org/10.3390/jof7070547

Camesasca, L., Ramírez, M. B., Guigou, M., Ferrari, M. D., & Lareo, C. (2015). Evaluation of dilute acid and alkaline pretreatments, enzymatic hydrolysis and fermentation of napiergrass for fuel ethanol production. *Biomass and Bioenergy*, *74*, 193–201. https://doi.org/10.1016/j.biombioe.2015.01.017

Chang, Y.-H., Chang, K.-S., Chen, C.-Y., Hsu, C.-L., Chang, T.-C., & Jang, H.-D. (2018). Enhancement of the Efficiency of Bioethanol Production by Saccharomyces cerevisiae via Gradually Batch-Wise and Fed-Batch Increasing the Glucose Concentration. *Fermentation*, *4*(2), 45. https://doi.org/10.3390/fermentation4020045

Chanpla, M., Kullavanijaya, P., Janejadkarn, A., & Chavalparit, O. (2018). Effect of harvesting age and performance evaluation on biogasification from Napier grass in separated stages process. *KSCE Journal of Civil Engineering*, *22*(1), 40–45. https://doi.org/10.1007/s12205-017-1164-y

Cheng, S., Huang, A., Wang, S., & Zhang, Q. (2016). Effect of Different Heat Treatment Temperatures on the Chemical Composition and Structure of Chinese Fir Wood. *BioResources*, *11*(2). https://doi.org/10.15376/biores.11.2.4006-4016

da Silva, A. S., Espinheira, R. P., Teixeira, R. S. S., de Souza, M. F., Ferreira-Leitão, V., & Bon, E. P. S. (2020). Constraints and advances in high-solids enzymatic hydrolysis of lignocellulosic biomass: a critical review. *Biotechnology for Biofuels*, *13*(1), 58. https://doi.org/10.1186/s13068-020-01697-w

Datta, R. (1981). Acidogenic fermentation of lignocellulose–acid yield and conversion of components. *Biotechnology and Bioengineering*, *23*(9), 2167–2170. https://doi.org/10.1002/bit.260230921

Ernawati, A., Abdullah, L., Permana, I. G., & Karti, P. D. M. H. (2023). Morphological responses, biomass production and nutrient of Pennisetum purpureum cv. Pakchong under different planting patterns and harvesting ages. *Biodiversitas Journal of Biological Diversity*, *24*(6). https://doi.org/10.13057/biodiv/d240640

Faix, O. (1991). Classification of Lignins from Different Botanical Origins by FT-IR Spectroscopy. *Holzforschung*, *45*(s1), 21–28. https://doi.org/10.1515/hfsg.1991.45.s1.21

Fornazier, M., de Oliveira Rodrigues, P., Pasquini, D., & Alves Baffi, M. (2025). Effects of Alkaline Pretreatment with Sodium Hydroxide with and Without Anthraquinone on the Enzymatic Hydrolysis of Corncob and Corn Stover and Ethanol Production. *Waste and Biomass Valorization*, *16*(5), 2535–2551. https://doi.org/10.1007/s12649-024-02811-x

Gao, Y., Xu, J., Yuan, Z., Jiang, J., Zhang, Z., & Li, C. (2018). Ethanol production from sugarcane bagasse by fed-batch simultaneous saccharification and fermentation at high solids loading. *Energy Science & Engineering*, *6*(6), 810–818. https://doi.org/10.1002/ese3.257

Hoyer, K., Galbe, M., & Zacchi, G. (2010). Effects of enzyme feeding strategy on ethanol yield in fed-batch simultaneous saccharification and fermentation of spruce at high dry matter. *Biotechnology for Biofuels*, *3*(1), 14. https://doi.org/10.1186/1754-6834-3-14

Hung, Y.-H. R., Chae, M., Sauvageau, D., & Bressler, D. C. (2023). Adapted feeding strategies in fed-batch fermentation improve sugar delivery and ethanol productivity. *Bioengineered*, *14*(1). https://doi.org/10.1080/21655979.2023.2250950

Hung, Y.-H. R., Sauvageau, D., & Bressler, D. C. (2025). An adaptive, continuous substrate feeding strategy based on evolved gas to improve fed-batch ethanol fermentation. *Applied Microbiology and Biotechnology*, *109*(1), 64. https://doi.org/10.1007/s00253-025-13447-9

IESR. (2024). Indonesia Energy Transition Outlook 2025: Navigating Indonesia's Energy Transition at the Crossroads: A Pivotal Moment for Redefining the Future. https://iesr.or.id/en/pustaka/indonesia-energy-transition-outlook-ieto-2025/

International Energy Agency. (2022). An Energy Sector Roadmap to Net Zero Emissions in Indonesia. In *An Energy Sector Roadmap to Net Zero Emissions in Indonesia*. https://doi.org/10.1787/4a9e9439-en

Kacuráková, M., & Wilson, R. H. (2001). Developments in mid-infrared FT-IR spectroscopy of selected carbohydrates. *Carbohydrate Polymers*, *44*(4), 291–303. https://doi.org/10.1016/S0144-8617(00)00245-9

Kongkeitkajorn, M. B., Yaemdeeka, R., Chaiyota, I., Hamsupo, K., Oraintara, A., & Reungsang, A. (2021). Bioethanol from Napier grass employing different fermentation strategies to evaluate a suitable operation for batch bioethanol production. *Energy Conversion and Management: X*, *12*, 100143. https://doi.org/10.1016/j.ecmx.2021.100143

Kottelat, J., Freeland, B., & Dabros, M. (2021). Novel Strategy for the Calorimetry-Based Control of Fed-Batch Cultivations of *Saccharomyces cerevisiae*. *Processes*, *9*(4), 723. https://doi.org/10.3390/pr9040723

Kristensen, J. B., Felby, C., & Jørgensen, H. (2009). Yield-determining factors in high-solids enzymatic hydrolysis of lignocellulose. *Biotechnology for Biofuels*, *2*(1), 11. https://doi.org/10.1186/1754-6834-2-11

Kumparan. (2023). Pertamax Green 95 Siap Dijual Pekan Depan, Tahap I di Jakarta & Surabaya. *KumparanBISNIS*.

Lara-Serrano, M., Morales-delaRosa, S., Campos-Martín, J. M., & Fierro, J. L. G. (2019). Fractionation of Lignocellulosic Biomass by Selective Precipitation from Ionic Liquid Dissolution. *Applied Sciences*, *9*(9), 1862. https://doi.org/10.3390/app9091862

Liu, Y., Xu, J., He, M., Liang, C., Yuan, Z., & Xie, J. (2016). Improved ethanol production based on high solids fed-batch simultaneous saccharification and fermentation with alkali-pretreated sugarcane bagasse. *BioRes*, *11*(1), 2548–2556.

Loedkunchotipat, K., Desclaux, S., & Maksup, S. (2015). Expression analysis of cellulose synthase and phenylalanine ammonia-lyase genes in Napier grass hybrids (Pennisetum hybrid). *Thai Journal of Genetics*, *8*, 167–174.

Lounglawan, P., Lounglawan, W., & Suksombat, W. (2014). Effect of Cutting Interval and Cutting Height on Yield and Chemical Composition of King Napier Grass (*Pennisetum purpureum* x *Pennisetum americanum*). *APCBEE Procedia*, *8*, 27–31. https://doi.org/10.1016/j.apcbee.2014.01.075

Lun, L. W., Gunny, A. A. N., Kasim, F. H., & Arbain, D. (2017). Fourier transform infrared spectroscopy (FTIR) analysis of paddy straw pulp treated using deep eutectic solvent. *AIP Conf. Proc.* 020049. https://doi.org/10.1063/1.4981871

Manokhoon, P., & Rangseesuriyachai, T. (2020). Effect of two-stage sodium hydroxide pretreatment on the composition and structure of Napier grass (Pakchong 1) (*Pennisetum purpureum*). *International Journal of Green Energy*, *17*(13), 864–871. https://doi.org/10.1080/15435075.2020.1809425

Meraj, A., Jawaid, M., Singh, S. P., Nasef, M. M., Ariffin, H., Fouad, H., & Abu-Jdayil, B. (2024). Isolation and characterisation of lignin using natural deep eutectic solvents pretreated kenaf fibre biomass. *Scientific Reports*, *14*(1), 8672. https://doi.org/10.1038/s41598-024-59200-6

Minmunin, J., Limpitipanich, P., & Promwungkwa, A. (2015). Delignification of Elephant Grass for Production of Cellulosic Intermediate. *Energy Procedia*, *79*, 220–225. https://doi.org/10.1016/j.egypro.2015.11.468

Olofsson, K., Bertilsson, M., & Lidén, G. (2008). A short review on SSF – an interesting process option for ethanol production from lignocellulosic feedstocks. *Biotechnology for Biofuels*, *1*(1), 7. https://doi.org/10.1186/1754-6834-1-7

Panakkal, E. J., Cheenkachorn, K., Chuetor, S., Tantayotai, P., Raina, N., Cheng, Y.-S., & Sriariyanun, M. (2022). Optimization of deep eutectic solvent pretreatment for bioethanol production from Napier grass. *Sustainable Energy Technologies and Assessments*, *54*, 102856. https://doi.org/10.1016/j.seta.2022.102856

Pandey, K. K., & Pitman, A. J. (2003). FTIR studies of the changes in wood chemistry following decay by brown-rot and white-rot fungi. *International Biodeterioration & Biodegradation*, *52*(3), 151–160. https://doi.org/10.1016/S0964-8305(03)00052-0

Pendse, D. S., Deshmukh, M., & Pande, A. (2023). Different pre-treatments and kinetic models for bioethanol production from lignocellulosic biomass: A review. *Heliyon*, *9*(6), e16604. https://doi.org/10.1016/j.heliyon.2023.e16604

Pensri, B., Aggarangsi, P., Chaiyaso, T., & Chandet, N. (2016). Potential of Fermentable Sugar Production from Napier cv. Pakchong 1 Grass Residue as a Substrate to Produce Bioethanol. *Energy Procedia*, *89*, 428–436. https://doi.org/10.1016/j.egypro.2016.06.287

Peraturan Presiden Nomor 40 Tahun 2023 Tentang Percepatan Swasembada Gula Nasional Dan Penyediaan Bioetanol Sebagai Bahan Bakar Nabati (Biofuel) (2023).

Phitsuwan, P., Sakka, K., & Ratanakhanokchai, K. (2016). Structural changes and enzymatic response of Napier grass (*Pennisetum purpureum*) stem induced by alkaline pretreatment. *Bioresource Technology*, *218*, 247–256. https://doi.org/10.1016/j.biortech.2016.06.089

Podkaminer, K. K., Kenealy, W. R., Herring, C. D., Hogsett, D. A., & Lynd, L. R. (2012). Ethanol and anaerobic conditions reversibly inhibit commercial cellulase activity in thermophilic simultaneous saccharification and fermentation (tSSF). *Biotechnology for Biofuels*, *5*(1), 43. https://doi.org/10.1186/1754-6834-5-43

Prasetyo, J., Akbar, M. A. B., Aulanni'am, Filailla, E., Dahnum, D., Maryana, R., Muryanto, M., Triwahyuni, E., Sudiyani, Y., Bardant, T. B., Irawan, Y., & Hirai, H. (2025). Optimizing for modified simultaneous saccharification and fermentation to produce bio-ethanol from environmentally friendly delignification of oil palm empty fruit bunch. *Biomass Conversion and Biorefinery*, *15*(4), 5303–5312. https://doi.org/10.1007/s13399-024-05435-2

Rahardjo, A. H., Azmi, R. M., Muharja, M., Aparamarta, H. W., & Widjaja, A. (2021). Pretreatment of Tropical Lignocellulosic Biomass for Industrial Biofuel Production: A Review. *IOP Conference Series: Materials Science and Engineering*, *1053*(1), 012097. https://doi.org/10.1088/1757-899X/1053/1/012097

Raspolli Galletti, A. M., D'Alessio, A., Licursi, D., Antonetti, C., Valentini, G., Galia, A., & Nassi o Di Nasso, N. (2015). Midinfrared FT-IR as a Tool for Monitoring Herbaceous Biomass Composition and Its Conversion to Furfural. *Journal of Spectroscopy*, *2015*, 1–12. https://doi.org/10.1155/2015/719042

Rengsirikul, K., Ishii, Y., Kangvansaichol, K., Sripichitt, P., Punsuvon, V., Vaithanomsat, P., Nakamanee, G., & Tudsri, S. (2013). Biomass Yield, Chemical Composition and Potential Ethanol Yields of 8 Cultivars of Napiergrass (*Pennisetum purpureum Schumach.*) Harvested 3-Monthly in Central Thailand. *Journal of Sustainable Bioenergy Systems*, *03*(02), 107–112. https://doi.org/10.4236/jsbs.2013.32015

Schwanninger, M., Rodrigues, J. C., Pereira, H., & Hinterstoisser, B. (2004). Effects of short-time vibratory ball milling on the shape of FT-IR spectra of wood and cellulose. *Vibrational Spectroscopy*, *36*(1), 23–40. https://doi.org/10.1016/j.vibspec.2004.02.003

Shadbahr, J., Khan, F., & Zhang, Y. (2017). Kinetic modeling and dynamic analysis of simultaneous saccharification and fermentation of cellulose to bioethanol. *Energy Conversion and Management*, *141*, 236–243. https://doi.org/10.1016/j.enconman.2016.08.025

Sun, R. C., Tomkinson, J., Ma, P. L., & Liang, S. F. (2000). Comparative study of hemicelluloses from rice straw by alkali and hydrogen peroxide treatments. *Carbohydrate Polymers*, *42*(2), 111–122. https://doi.org/10.1016/S0144-8617(99)00136-8

Tarasov, D., Leitch, M., & Fatehi, P. (2018). Lignin–carbohydrate complexes: properties, applications, analyses, and methods of extraction: a review. *Biotechnology for Biofuels*, *11*(1), 269. https://doi.org/10.1186/s13068-018-1262-1

Wang, Z., Lv, Z., Yang, X., & Tian, S. (2013). Fed-batch mode optimization of SSF for cellulosic ethanol production from steam-exploded corn stover. *BioRes*, *8*(4), 5773–5782.

Xiao, Z., Zhao, Y., Wang, Y., Tan, X., Wang, L., Mao, J., Zhang, S., Lu, Q., Hu, F., Zuo, S., Liu, J., & Shan, Y. (2025). Sucrose-driven carbon redox rebalancing eliminates the Crabtree effect and boosts energy metabolism in yeast. *Nature Communications*, *16*(1), 5211. https://doi.org/10.1038/s41467-025-60578-8

Xie, Y., Hill, C. A. S., Xiao, Z., Militz, H., & Mai, C. (2010). Silane coupling agents used for natural fiber/polymer composites: A review. *Composites Part A: Applied Science and Manufacturing*, *41*(7), 806–819. https://doi.org/10.1016/j.compositesa.2010.03.005

Yasuda, M., Nagai, H., Takeo, K., Ishii, Y., & Ohta, K. (2014). Bio-ethanol production through simultaneous saccharification and co-fermentation (SSCF) of a low-moisture anhydrous ammonia (LMAA)-pretreated napiegrass (*Pennisetum purpureum Schumach*). *SpringerPlus*, *3*(1), 333. https://doi.org/10.1186/2193-1801-3-333

Zhuang, J., Li, M., Pu, Y., Ragauskas, A., & Yoo, C. (2020). Observation of Potential Contaminants in Processed Biomass Using Fourier Transform Infrared Spectroscopy. *Applied Sciences*, *10*(12), 4345. https://doi.org/10.3390/app10124345